buildings

MDPI

Article

New Fuzzy-Heuristic Methodology for Analyzing Compression Load Capacity of Composite Columns

Bizhan Karimi Sharafshadeh [1], Mohammad Javad Ketabdari [2,†], Farhood Azarsina [3], Mohammad Amiri [4] and Moncef L. Nehdi [5,*]

[1] Department of Civil Engineering, Qeshm Branch, Islamic Azad University, Qeshm 79515/1393, Iran
[2] Department of Maritime Engineering, Amirkabir University of Technology, Tehran 1591634311, Iran
[3] Department of Marine Structures, Science and Research Branch, Islamic Azad University, Tehran 14515/775, Iran
[4] Faculty of Engineering, University of Hormozgan, Bandar Abbas 7916193145, Iran
[5] Department of Civil Engineering, McMaster University, Hamilton, ON L8S 4L8, Canada
* Correspondence: nehdim@mcmaster.ca
† Deceased author.

Abstract: Predicting the mechanical strength of structural elements is a crucial task for the efficient design of buildings. Considering the shortcomings of experimental and empirical approaches, there is growing interest in using artificial intelligence techniques to develop data-driven tools for this purpose. In this research, empowered machine learning was employed to analyze the axial compression capacity (CC) of circular concrete-filled steel tube (CCFST) composite columns. Accordingly, the adaptive neuro-fuzzy inference system (ANFIS) was trained using four metaheuristic techniques, namely earthworm algorithm (EWA), particle swarm optimization (PSO), salp swarm algorithm (SSA), and teaching learning-based optimization (TLBO). The models were first applied to capture the relationship between the CC and column characteristics. Subsequently, they were requested to predict the CC for new column conditions. According to the results of both phases, all four models could achieve dependable accuracy. However, the PSO-ANFIS was tangibly more efficient than the other models in terms of computational time and accuracy and could attain more accurate predictions for extreme conditions. This model could predict the CC with a relative error below 2% and a correlation exceeding 99%. The PSO-ANFIS is therefore recommended as an effective tool for practical applications in analyzing the behavior of the CCFST columns.

Keywords: composite elements; CCFSTC columns; compression capacity; machine learning; optimization algorithms

Citation: Karimi Sharafshadeh, B.; Ketabdari, M.J.; Azarsina, F.; Amiri, M.; Nehdi, M.L. New Fuzzy-Heuristic Methodology for Analyzing Compression Load Capacity of Composite Columns. *Buildings* **2023**, *13*, 125. https://doi.org/10.3390/buildings13010125

Academic Editor: Ahmed Senouci

Received: 12 November 2022
Revised: 14 December 2022
Accepted: 19 December 2022
Published: 3 January 2023

1. Introduction

Concrete and steel are the most fundamental materials needed for today's construction [1–3]. Since they can withstand significant amounts of stress (e.g., compression, tension, shear, etc.), engineers design structural components such as columns and beams using concrete and steel [4,5]. Owing to this popularity, researchers have always studied their various mechanical characteristics [6–8]. A proper combination of these two materials results in composite materials, e.g., concrete-filled steel tubular elements, which are suitable choices for a wide variety of civil engineering projects [9]. These elements can play a role in structures such as bridges [10], wharves [11], and roadways [12]. As a broadly used structural element, circular concrete-filled steel tube (CCFST) columns are attracting increasing attention in the building sector. These columns synthesize the best characteristics of both concrete and steel materials which makes them more desirable than separate ones. This combination not only improves the concrete in terms of toughness and plasticity but can help avoid (or delay) the local buckling of the steel [13]. High ductility, high strength, and high stiffness are mentioned as the most notable merits of the CCFST column [14].

So far, many researchers have presented valuable solutions using numerical and analytical techniques for analyzing the behavior of the CCFST columns [15–17]. Among the different characteristics of these columns, axial compression capacity (CC) has received special attention [18,19]. Yu et al. [20] proposed an analytical-based unified formula for estimating the CC of the CCFST columns. Their validations proved that this formula can properly work for calculating the bearing capacity of both hollow and solid columns. Wu et al. [21] conducted an experimental study to investigate the compressive behavior of CCFST column with a focus on the effect of (a) the replacement ratio of demolished concrete lumps, (b) the strength of the fresh concrete, (c) the thickness of the steel tubes, and (d) the distribution of steel stirrups. Abdalla et al. [22] studied the compressive response of these columns under quasi-static loads and reported the effect of several parameters on the capacity of the columns. It is true that all such efforts provide valuable findings for developing more efficient CCFST columns, but they suffer from important demerits such as being costly and time consuming. Further, obtaining results in many cases entails performing destructive laboratory tests. This is while more recent studies have put their focus on much more efficient approaches that are capable of coping with non-linear calculations [23]. Machine learning models have nicely served for estimating many parameters in civil engineering [24–26]. Not surprisingly, concrete-related parameters, too, are being promisingly modeled using machine learning [27,28].

Having a finer focus on the prediction of CC for CCFST columns, intelligent models have properly dealt with this problem. Many engineers have employed predictive tools such as artificial neural networks (ANN) and adaptive neuro-fuzzy inference systems (ANFIS) for this purpose [29,30]. Basarir et al. [31] applied an ANFIS model to predict the pure bending capacity of concrete-filled steel tubes. Their findings revealed the superiority of this model over regression-based tools. Ho and Le [32] investigated and proved the competency of regression machine learning techniques for analyzing the ultimate load of CCFST columns whose experimental data are subjected to variability. They extracted an Excel-based equation from the most accurate model. Tran et al. [33] designed a convenient ANN-based GUI for predicting the axial CC of the CCFST columns.

It is a well-known fact that machine learning models can deal with almost any prediction task. Going beyond this, recent studies have shown that intelligent models can even experience improvements. One approach is to use a qualified metaheuristic algorithm to handle the training stage. Accordingly, programmers have developed hybrid models for engineering tasks. Zhao et al. [34] could optimize the ANN using a so-called metaheuristic technique, "equilibrium optimizer," to predict the splitting tensile strength of concrete. The prediction error of the ANN decreased by around 11.5% after incorporating it with the equilibrium optimization (EO). Lyu et al. [35] achieved an optimal configuration of the support vector regression model by hybridizing it with a sine–cosine algorithm. This model was tested for the problem of CC prediction, and their findings indicated the competency of this hybrid model as a design assistant, while empirical formulas could not comply with the sufficient condition. Luat et al. [36] suggested and tested the combination of a so-called machine learning model "Bayesian additive regression tree (BART)" with genetic algorithm (GA), artificial bee colony (ABC), and particle swarm optimization (PSO) metaheuristic techniques for modeling the axial load capacity. The prediction results corresponding to these hybrids achieved coefficients of determination equal to 0.9891, 0.9923, and 0.9931, respectively.

Complicated problems such as analyzing CCFST columns call for assessing new approaches to keep the solutions updated with the latest computational developments. Following the wide application of metaheuristic algorithms in creating powerful hybrid models in solving complicated problems, some new members of this family are examined in this study. On the other hand, previous efforts have mostly focused on ANNs as the to-be-optimized predictive model [13,37,38], and accordingly, it can be argued that the potential of leading models such as ANFIS needs further investigation. Hence, to bridge the mentioned gaps of knowledge, the main contributions of this study can be drawn on the following aspects: (a) introducing and evaluating the performance of novel

artificial intelligence-based hybrids for predicting the CC of CCFST columns, (b) utilizing ANFIS as the basic skeleton of the suggested models, and (c) comparing the efficiency of three metaheuristic optimizers, namely earthworm algorithm (EWA), salp swarm algorithm (SSA), and teaching learning-based optimization (TLBO) versus the PSO algorithm for adjusting the internal parameters of ANFIS. The findings of this study reflect efficient and applicable methodologies for enhancing the design of CCFST columns. As is known, a reliable indirect approximator can be of great interest to structural engineers due to the cost- and time-efficiency, as well as the easiness of implementation.

2. Data Provision

It was earlier explained that the axial CC of the CCFST columns is a complex non-linear parameter. In studies performed so far, this parameter has been considered as a function of several geometrical and material-related factors. These factors here comprise the length of column (L), the diameter (D), thickness (t), yield stress (f_y), and ultimate stress (f_u) of the steel tube, as well as the compressive strength of UHSC (f_c'). The used data are obtained from a study by Tran, Thai, and Nguyen [33]. They created a numerical dataset as the result of an extensive finite element simulation verified with experimental efforts in the literature. The readers are guided to refer to the reference paper [33] for further details of data provision (e.g., material characteristics, assumptions of simulation, parameters, etc.).

Figure 1 depicts how the CC values on the y-axis are in a relationship with these influential parameters. The values of CC range from 8016.3 to 75,051.6 kN, while the values of L, D, t, f_y, f_u, and f_c' fall within (900.0, 4800.0) mm, (300.0, 600.0) mm, (6.0, 30.0) mm, (235.0, 460.0) MPa, (360.0, 540.0) MPa, and (100.0, 200.0) MPa, respectively. An R-value is also calculated for each chart that shows the correlation between the CC and corresponding input. As is seen, the sole meaningful relationship here is between the CC and D with R = 0.90703. Other R values are below 0.5. Moreover, Table 1 gives some statistical details of the used dataset.

According to the sensitivity analysis carried out by Zheng et al. [39] on this dataset, the D and f_c' are the most important parameters for predicting the CC, while the lowest importance is obtained for the f_u and L.

In the prediction of CC using artificial intelligence models, the CC is the output of the model, while the named influential factors (L, D, t, f_y, f_u, and f_c') are referred to as the inputs of the network. The used data consist of 768 records that are divided into two sets after permuting their order. This is performed to achieve a random division. The first set of data, which contains 80% of the whole, is devoted to the training process. In other words, the network goes through these data to learn the mathematical relationship between the CC and inputs. The second set, which contains the remaining 20%, will be later used as non-processed data to evaluate the prediction ability of the models. This process is called the testing phase. In both the training and testing phases, the real values of CC are compared with the products of the models for accuracy evaluation.

Table 1. Statistical analysis of the CC and influential factors.

Indicator	Factor						
	L [mm]	D [mm]	t [mm]	f_y [MPa]	f_u [MPa]	f_c' [MPa]	CC [kN]
Mean	2475.0	450.0	15.2	331.3	460.0	150.0	30,185.3
Std. Error	47.4	4	0.2	3.1	2.5	1.2	538.3
Std. Deviation	1313.1	111.9	6.1	86	70.4	34.2	14,918.5
Sample Variance	1,724,120	12,516.3	37.3	7401.8	4956.5	1168.2	222,561,708.9
Minimum	900.0	300.0	6.0	235.0	360.0	100.0	8016.3
Maximum	4800.0	600.0	30.0	460.0	540.0	200.0	75,051.6

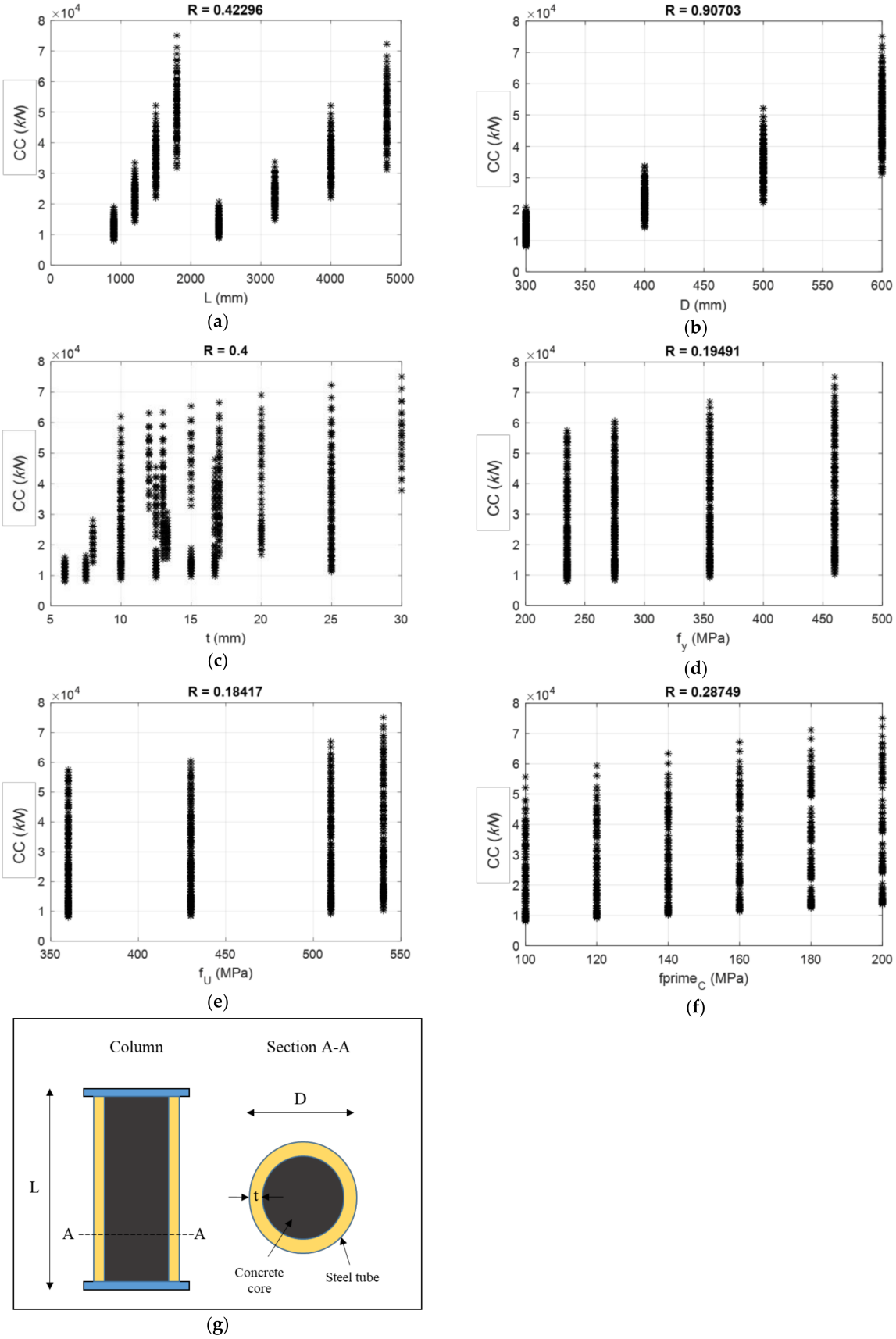

Figure 1. The distribution of the CC versus influential factors (**a**) L, (**b**) D, (**c**) t, (**d**) f_y, (**e**) f_u, and (**f**) f_c' and (**g**) a schematic view of the column and section.

3. Methodology

3.1. ANFIS

Jang [40] designed ANFIS as a hybrid type of artificial model. It is a universal approximator that takes advantage of both ANN and fuzzy inference systems. The mutual association of these two models results in the betterment of their performance. Fuzzy rules are considered in ANFIS to map the dependency of output on input parameters. Although ANFIS is capable of solving problems by taking human reasoning in linguistic terms, the ANN can complete its ability to derive rules from data [41].

The prediction using the ANFIS model draws on five layers. In the first one, the model computes the membership values for input factors. In so doing, the coefficients of membership functions (MFs) are adjusted as premise parameters. In the next layer, a power value is calculated for each derived rule in the nonadaptive nodes. Each power value is then normalized in the third layer based on the values calculated in the former layer. Following this, a first-order polynomial and normalized powers are multiplied in the fourth layer. Note that the coefficients for this polynomial are obtained by a recursive least-square technique. In the last layer, there is only one nonadaptive node, such as those in layers 2 and 3, which calculates a weighted average of its inputs to release the global response of the ANFIS. More details regarding the mathematical strategy of the ANFIS can be found in earlier literature [42,43].

3.2. Metaheuristic Algorithms

Metaheuristic algorithms are wise optimizers [44,45] that have recently drawn huge attention in various fields, especially engineering simulations. When it comes to an optimization problem, one (or more) product is expected to be maximized against the cost. This task can be efficiently handled by these algorithms. Most metaheuristic optimizers are nature-inspired. In other words, they simulate a natural behavior in order to reach the optimal solution to a given problem. In this work, four capable algorithms of EWA, PSO, SSA, and TLBO are used in combination with ANFIS to optimally analyze the compression-bearing capacity of the CCFST columns.

As explained, a metaheuristic algorithm needs to be applied to a problem. When coupled with ANFIS, the optimization problem becomes tuning the parameters of MFs so that the error of prediction is minimized. Simply speaking, the algorithm plays the role of the trainer for the ANFIS network [46].

The EWA mimics the reproduction behavior of earthworms. Wang et al. [47] designed this algorithm to present a new optimization method. It is known that one earthworm can perform the reproduction process alone. There are three fundamental assumptions regarding the reproduction process: (a) offsprings are produced by each earthworm by two and only two reproduction types, (b) both parent and corresponding child carry the same length genes, and (c) a number of best-fitted earthworms move forward directly to the subsequent without experiencing any change. Conceptually, the steps of the EWA algorithm comprise Reproduction 1, Reproduction 2, Weighted Summation, and a Cauchy mutation process for escaping from the local optimum. Further details regarding this algorithm can be found in [48,49].

The name PSO signifies a powerful optimization strategy that was introduced by Eberhart and Kennedy [50]. The PSO is a simulation of the real-world swarm movement of animals (e.g., birds flocking). The solutions of this algorithm are particles that, having a leader–follower relationship, fly within the space to improve their fitness. Accordingly, two parameters of local and global fitness are calculated and updated successively. Although the PSO belongs to the first generations of metaheuristic algorithms, it enjoys computationally significant advantages such as faster convergence and also demands less memory [51]. So far, this algorithm has been promisingly combined with conventional predictive models such as ANFIS. More explanations about the optimization mechanism of the PSO can be found in earlier literature [52,53].

The next algorithm used in this study is the SSA. It was presented by Mirjalili et al. [54] based on the foraging social behavior of the so-called tunicate "salp". Salp is a member of the Salpidae family that has a barrel shape. They live in chains, in which a follower population follows a leader toward a potential food source to improve the individuals' position, and, consequently, the solution to the problem. This algorithm hires several stochastic operators that enable it to stay away from local minima in multi-modal spaces. Hence, it can be mentioned among the most capable nature-inspired optimization techniques. For mathematical details of the SSA algorithm, recent studies such as [55,56] are suggested.

The TLBO algorithm was developed by Rao et al. [57]. This algorithm simulates the tutoring interaction between the teacher and students in a virtual class. The goal of the algorithm is to organize the best harmony within the class. It happens over two phases dedicated to teaching and learning. In the first phase, the most outstanding student is selected as the teacher. The teacher then tries to enhance the class by sharing knowledge. In the next phase, the students perform active interactions to share knowledge. This process results in improving the solution over an iterative process. As an advantage, implementing the TLBO algorithm does not require adjusting different hyperparameters [58]. This algorithm is better detailed in studies such as [59,60].

4. Results and Discussion

Accuracy assessment is the most significant step for evaluating the performance of the predictive models. However, other criteria, such as time efficiency and the simplicity of model configuration, are also of high importance. As used in many previous works, evaluation of the accuracy needs more than one criterion. It is more highlighted for comparative works wherein several models need to be relatively assessed.

In this work, the error of prediction is originally measured via the root mean square error (*RMSE*) and mean absolute error (*MAE*). Moreover, a relative form of MAE called mean absolute percentage error (*MAPE*) is also calculated to give a relative representation of the error [61,62].

$$RMSE = \sqrt{\frac{1}{J}\sum_{j=1}^{J}[Err_j]}^{2} \quad (1)$$

$$MAE = \frac{1}{J}\sum_{j=1}^{J}|Err_j| \quad (2)$$

$$MAPE = \frac{1}{J}\sum_{j=1}^{J}\left|\frac{Err_j}{CC_{j_{observed}}}\right| \times 100 \quad (3)$$

where the simple difference between the target CC ($CC_{j_{observed}}$) and simulated CC ($CC_{j_{simulated}}$) is referred to as Err_j and is calculated as follows:

$$Err_j = CC_{j_{observed}} - CC_{j_{simulated}} \quad (4)$$

Needless to say, all error criteria give the difference between the target and output values. A correlation criterion quantifies the compatibility of these values. This compatibility is here measured using the Pearson correlation coefficient (*R*).

$$R = \frac{\sum_{j=1}^{J}(CC_{j_{simulated}} - \overline{CC}_{simulated})(CC_{j_{observed}} - \overline{CC}_{observed})}{\sqrt{\sum_{j=1}^{J}(CC_{j_{simulated}} - \overline{CC}_{simulated})^2}\sqrt{\sum_{i=1}^{N}(CC_{j_{observed}} - \overline{CC}_{observed})^2}} \quad (5)$$

where $\overline{CC}$ stands for the average of the corresponding CC values.

4.1. Metaheuristic Optimization

This step stands for the training process of the ANFIS model. The difference with normal training is the used algorithm and, consequently, the strategy for adjusting the MF parameters. In so doing, the raw network becomes the optimization case of the metaheuristic algorithms (i.e., EWA, PSO, SSA, and TLBO), and the algorithm tries to train the model based on the training data. During an iterative process, numerous configurations are tried for the MF parameters so that the learning quality increases over and over. In this work, each of the hybrid models, i.e., EWA-ANFIS, PSO-ANFIS, SSA-ANFIS, and TLBO-ANFIS, are implemented with 1000 iterations. The quality of the result is monitored by calculating the RMSE in each iteration.

On the other hand, when it comes to metaheuristic algorithms, a so-called parameter "population size" emerges as an effective factor. It is because these techniques pursue the optimal solution by means of search agents. Hence, the number of agents can influence the solution in terms of quality and convergence speed. This study uses a trial-and-error sequence to investigate the effect of population size. The tested values include 10, 25, 50, 100, 200, 300, 400, and 500. The results of this process (i.e., the final RMSE values) are shown in the column chart of Figure 2.

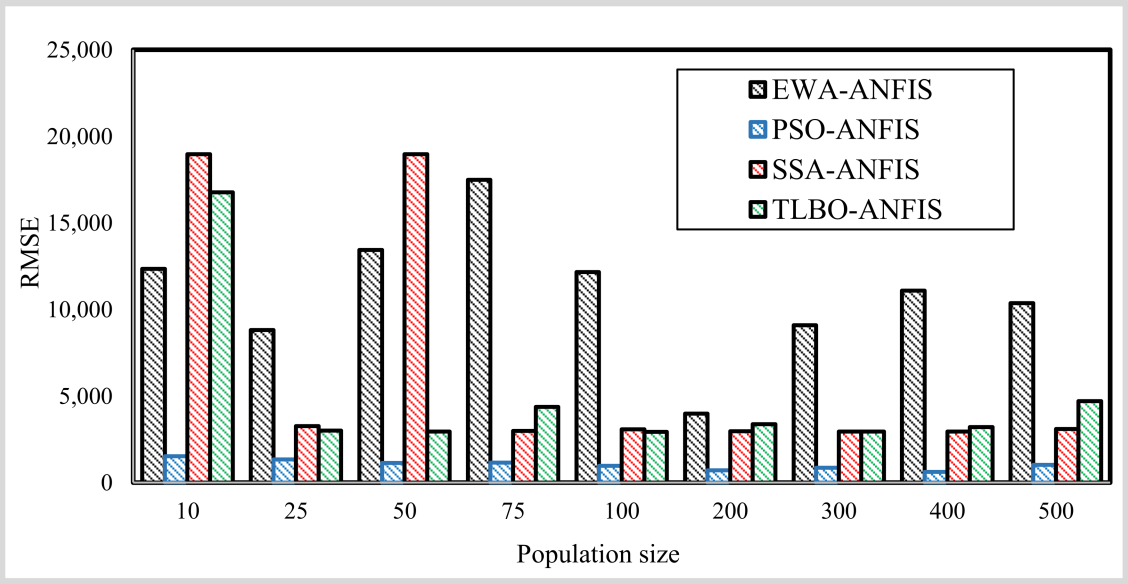

Figure 2. The trial-and-error results for selecting the best population size.

As is seen, a stochastic behavior is exhibited by the networks. However, at a glance, the right-hand side columns indicate lower RMSE, meaning that the models have better performance for larger population sizes. Further, a significant difference can be observed between the columns corresponding to the PSO-ANFIS and the other three models. According to Figure 2, the best quality of training resulted in population sizes of 200, 400, 400, and 100 for the EWA-ANFIS, PSO-ANFIS, SSA-ANFIS, and TLBO-ANFIS, respectively. Hereupon, these networks demonstrate the results for further evaluation and comparisons.

Figure 3 shows the optimization curves of the mentioned model. As is seen, each model goes through a different path to minimize the error. What is clearly derived from this figure is the sufficiency of 1000 iterations for optimizing the ANFIS using the EWA, PSO, SSA, and TLBO. This claim is based on the steady optimization behavior of all algorithms after the 800th iteration. In the end, the EWA-ANFIS, PSO-ANFIS, SSA-ANFIS, and TLBO-ANFIS achieved the RMSEs of 3984.7939, 618.2641, 2950.3632, and 2923.1084, respectively. Considering the optimization time, implementation of the EWA-ANFIS with 1538.1 s was the longest one, followed by the SSA-ANFIS with 1122.8 s, TLBO-ANFIS with 542.7 s, and

PSO-ANFIS with 388.8 s. An HP Intel Core i7 64-bit operating system with 16 GB of RAM was used for this study.

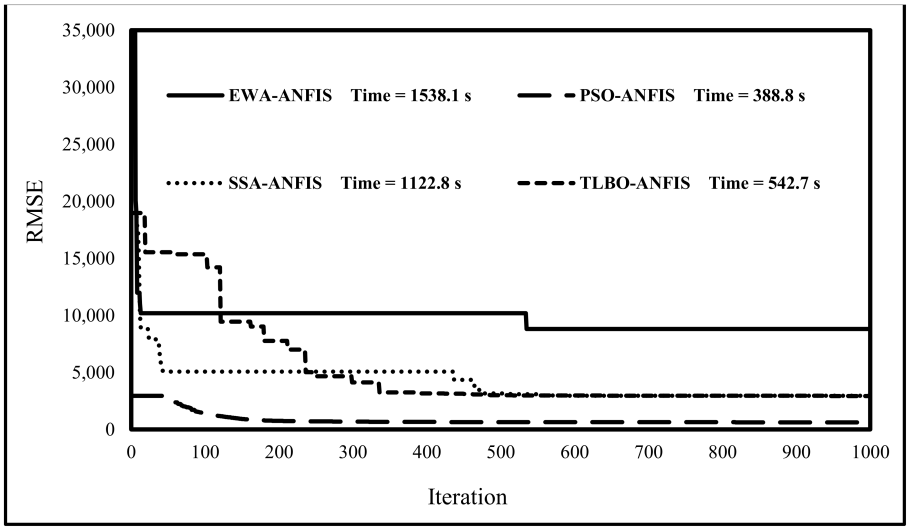

Figure 3. Metaheuristic-based optimization curves of the ANFIS.

4.2. Prediction Results

Focusing on the training results, all models attained a suitable understanding of the relationship between the CC and L, D, t, f_y, f_u, and f_c'. Apart from the reported RMSEs, the MAEs of 3085.0588, 466.4530, 2296.0564, and 2282.5048 indicate a fine level of learning error. Figure 4 depicts the histogram of the training *Err* values (see Equation (4)).

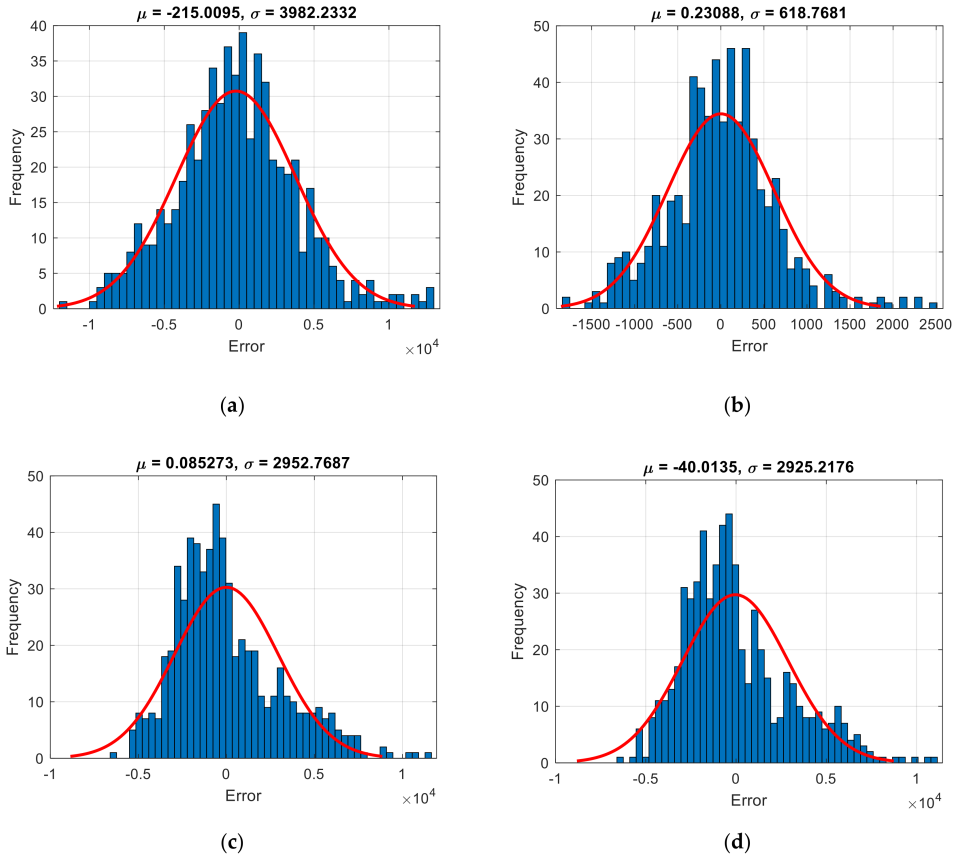

Figure 4. Histogram of the errors obtained for (**a**) EWA-ANFIS, (**b**) PSO-ANFIS, (**c**) SSA-ANFIS, and (**d**) TLBO-ANFIS.

Based on this figure, as well as the MAPE values equal to 12.4133, 1.8477, 10.3899, and 10.2947%, the error of all four models is at an acceptable level. It reflects the high ability of the EWA, PSO, SSA, and TLBO in tuning the MF parameters of the ANFIS. This goodness of the performance can be certified with high correlation values, i.e., R index equal to 0.96436, 0.99915, 0.98055, and 0.98092.

From the training results, it was concluded that the models could predict the CC of experienced conditions with a high level of accuracy. However, for the overall judgment, they were exposed to new conditions that had not been analyzed before, i.e., testing data. Having 20% of 768 data, the condition of 154 CCFST columns was given to the trained models for predicting the corresponding CCs. This prediction was associated with RMSEs of 4033.8367, 744.1464, 2874.7402, and 2854.8094, as well as the MAEs of 12.9215, 1.9996, 10.6235, and 10.4921. Relative to the range of the observed CCs (i.e., 8016.3 to 75,051.6 N), the prediction errors are tolerable and indicate the reliability of all four models for the CC modeling. In detail, the relative errors were 12.9215, 1.9996, 10.6235, and 10.4921 in terms of the MAPE.

Furthermore, the correlation assessment of the testing results is depicted in Figure 5, wherein the observed values (on the *x*-axis) are compared to simulated values (on the *y*-axis). Hence, the ideal situation happens for data that are located on the line x = y. According to these illustrations, the products of the fuzzy networks are in suitable agreement with reality. The R values of 0.96106, 0.99868, 0.98004, and 0.98037 can certify a desirable correlation for all four models.

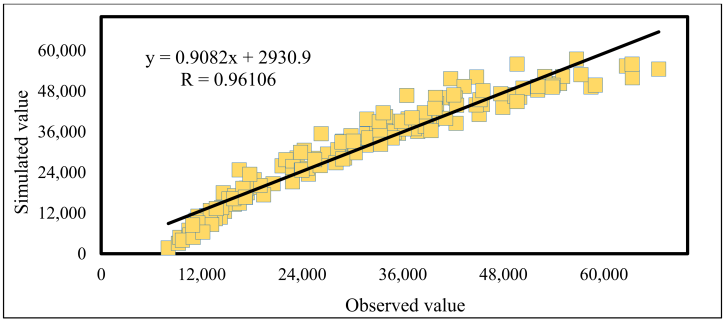

(a)

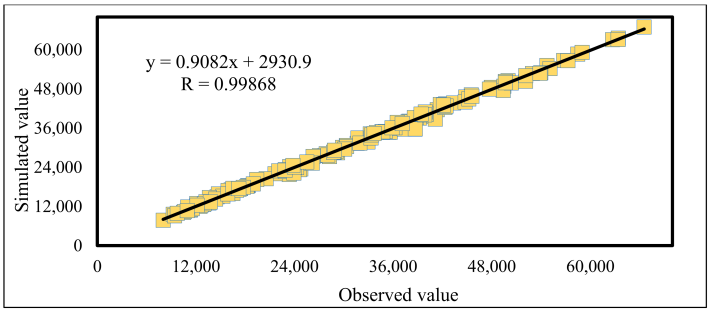

(b)

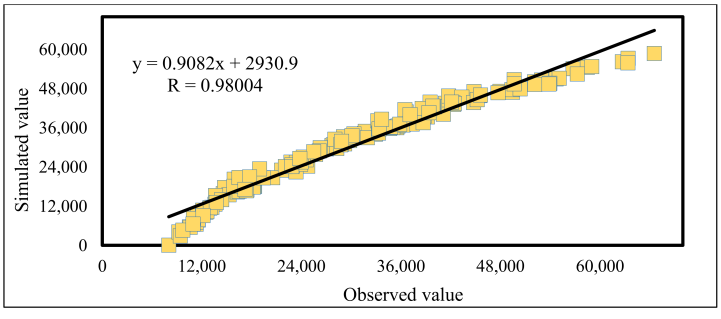

(c)

Figure 5. *Cont.*

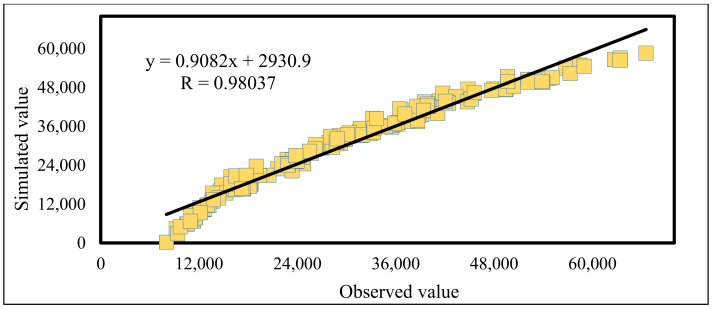

(**d**)

Figure 5. Correlation assessment of the testing data for (**a**) EWA-ANFIS, (**b**) PSO-ANFIS, (**c**) SSA-ANFIS, and (**d**) TLBO-ANFIS.

4.3. Comparison

Previous assessments showed that all four models of EWA-ANFIS, PSO-ANFIS, SSA-ANFIS, and TLBO-ANFIS are suitable fuzzy approaches for predicting the axial CC of the CCFST columns. However, there were significant distinctions between the performance of these four models. More clearly, the EWA-ANFIS was characterized by the largest error and lowest correlation, while the PSO-ANFIS presented the best accuracy of prediction. Relative to these two models, the SSA-ANFIS and TLBO-ANFIS emerged to have very close accuracy (with less than 1% of difference); however, the TLBO-based model was superior. Therefore, from the accuracy point of view, the PSO-ANFIS was the most reliable model, followed by the TLBO-ANFIS, SSA-ANFIS, and EWA-ANFIS.

It is worth mentioning that, in the case of EWA-ANFIS and PSO-ANFIS, the training results were of higher accuracy, whereas for the two other models (i.e., SSA-ANFIS and TLBO-ANFIS), there were superiorities in terms of used accuracy indices. For instance, while the testing RMSE of the TLBO-ANFIS is below the training one (2923.1084 vs. 2854.8094), the training MAE shows a smaller error than the testing phase (2282.5048 vs. 2312.5851).

As visual reasoning, the correlation charts given in Figure 5 can be considered for comparing the prediction potential of the used models. It is true that, in comparison with the EWA-ANFIS, the data of three other models are better aggregated around the ideal line, but there is a significant difference between the PSO-ANFIS and two other fuzzy tools. It is immediately clear that the SSA-ANFIS and TLBO-ANFIS, despite their outstanding potential, still have weaknesses in dealing with extremum CC values. In other words, the maximum and minimum CC data are a little deviated from the general trend. This shortcoming is nicely covered by the PSO-ANFIS.

Time efficiency is another appreciable factor for comparing the capacity of the models. It is explained in Figure 3 that the PSO-ANFIS elapsed in the shortest time among the used models. Moreover, the convergence curves show that the PSO algorithm can reach a stable, yet optimum, solution faster. Generally speaking, it enjoys a higher convergence speed.

All in all, the PSO-ANFIS can be selected as the most optimum hybrid among those evaluated in this research. Utilizing the PSO algorithm provided a faster and tangibly more accurate solution to the problem of CC prediction. This algorithm benefitted from a natural swarm behavior to tune the MF parameters of the fuzzy model with respect to a complex relationship between the CC and L, D, t, f_y, f_u, and f_c'. The corresponding hybrid tool, i.e., PSO-ANFIS, can be introduced as a reliable and efficient predictive model for this purpose.

5. Conclusions

The application of four optimal hybrid tools was tested for predicting the compression capacity of circular concrete-filled steel tube columns made with ultra-high-strength concrete. The models were composed of two parts: (a) a conventional ANFIS framework, and (b) one of the following optimizers: earthworm algorithm, particle swarm optimization, salp swarm algorithm, and teaching learning-based optimization. The models were trained using the finite element-based data of earlier work. The main results are as follows:

- Metaheuristic algorithms are suitable options for training neuro-fuzzy systems for the mentioned purpose.
- Referring to the correlation values >0.96, all employed fuzzy-metaheuristic models are capable of both comprehending and generalizing the relationship between the CC and input parameters.
- The PSO algorithm emerged as the most suitable optimizer for the ANFIS. This deduction came up due to the highest accuracy, as well as the most time-efficient optimization behavior observed compared to the three other algorithms.
- The PSO-ANFIS could present a finer prediction of extremum CC values.
- In short, the use of the PSO-ANFIS is recommended for practical applications which pursue efficient cost-competitive design of CCFST columns.

Author Contributions: Conceptualization: M.J.K., F.A., M.A. and M.L.N.; methodology: B.K.S., M.J.K., F.A. and M.A.; software and validation: B.K.S., M.J.K., F.A., M.A. and M.L.N.; formal analysis and investigation: B.K.S., F.A. and M.A.; data curation: B.K.S.; writing—original draft preparation: B.K.S., M.J.K., F.A. and M.A.; writing—review and editing, M.J.K. and M.L.N.; visualization: B.K.S., M.J.K., F.A. and M.A.; supervision and project administration: M.J.K. and M.L.N. All authors have read and agreed to the published version of the manuscript.

Funding: This research received no external funding.

Data Availability Statement: The database used in the development of this work could be obtained from the corresponding author after an embargo period.

Conflicts of Interest: The authors declare no conflict of interest.

Nomenclature

CCFST	Circular concrete-filled steel tube	CC	Compression capacity
ANN	Artificial neural network	ANFIS	Adaptive neuro-fuzzy inference system
BART	Bayesian additive regression tree	GA	Genetic algorithm
ABC	Artificial bee colony	PSO	Particle swarm optimization
EWA	Earthworm algorithm	SSA	Salp swarm algorithm
TLBO	Teaching learning-based optimization	f_c'	Compressive strength of UHSC
L	Length of column	D	Diameter
t	Thickness	f_y	Yield stress
f_u	Ultimate stress of the steel tube	MF	Membership function
RMSE	Root mean square error	R	Pearson correlation index
MAPE	Mean absolute percentage error	MAE	Mean absolute error

References

1. Zhang, Z.; Liang, G.; Niu, Q.; Wang, F.; Chen, J.; Zhao, B.; Ke, L. A Wiener degradation process with drift-based approach of determining target reliability index of concrete structures. *Qual. Reliab. Eng. Int.* **2022**, *38*, 3710–3725. [CrossRef]
2. Zhang, H.; Li, L.; Ma, W.; Luo, Y.; Li, Z.; Kuai, H. In Effects of welding residual stresses on fatigue reliability assessment of a PC beam bridge with corrugated steel webs under dynamic vehicle loading. *Structures* **2022**, *45*, 1561–1572. [CrossRef]
3. Zhang, C.; Ali, A.; Sun, L. Investigation on low-cost friction-based isolation systems for masonry building structures: Experimental and numerical studies. *Eng. Struct.* **2021**, *243*, 112645.
4. Huang, Y.; Zhang, W.; Liu, X. Assessment of Diagonal Macrocrack-Induced Debonding Mechanisms in FRP-Strengthened RC Beams. *J. Compos. Constr.* **2022**, *26*, 04022056. [CrossRef]
5. Huang, H.; Yao, Y.; Liang, C.; Ye, Y. Experimental study on cyclic performance of steel-hollow core partially encased composite spliced frame beam. *Soil Dyn. Earthq. Eng.* **2022**, *163*, 107499. [CrossRef]
6. Liao, D.; Zhu, S.-P.; Keshtegar, B.; Qian, G.; Wang, Q. Probabilistic framework for fatigue life assessment of notched components under size effects. *Int. J. Mech. Sci.* **2020**, *181*, 105685.
7. He, J.-C.; Zhu, S.-P.; Luo, C.; Niu, X.; Wang, Q. Size effect in fatigue modelling of defective materials: Application of the calibrated weakest-link theory. *Int. J. Fatigue* **2022**, *165*, 107213. [CrossRef]
8. Xu, H.; He, T.; Zhong, N.; Zhao, B.; Liu, Z. Transient thermomechanical analysis of micro cylindrical asperity sliding contact of SnSbCu alloy. *Tribol. Int.* **2022**, *167*, 107362. [CrossRef]
9. Han, L.-H.; Li, W.; Bjorhovde, R. Developments and advanced applications of concrete-filled steel tubular (CFST) structures: Members. *J. Constr. Steel Res.* **2014**, *100*, 211–228. [CrossRef]

10. Yang, M.-G.; Cai, C.; Chen, Y. Creep performance of concrete-filled steel tubular (CFST) columns and applications to a CFST arch bridge. *Steel Compos. Struct.* **2015**, *19*, 111–129. [CrossRef]
11. Lin, L.; Wang, F. A finite element based study on concrete filled steel tube (CFST) pile used in wharf structure. In Proceedings of the 32nd International Ocean and Polar Engineering Conference, Shanghai, China, 6–10 June 2022; OnePetro: Richardson, TX, USA, 2022.
12. Zhang, J.; Liu, L.; Cao, J.; Yan, X.; Zhang, F. Mechanism and application of concrete-filled steel tubular support in deep and high stress roadway. *Constr. Build. Mater.* **2018**, *186*, 233–246. [CrossRef]
13. Ren, Q.; Li, M.; Zhang, M.; Shen, Y.; Si, W. Prediction of ultimate axial capacity of square concrete-filled steel tubular short columns using a hybrid intelligent algorithm. *Appl. Sci.* **2019**, *9*, 2802. [CrossRef]
14. Dundu, M. Compressive strength of circular concrete filled steel tube columns. *Thin-Walled Struct.* **2012**, *56*, 62–70. [CrossRef]
15. Zhai, Q.; Zhang, J.; Xiao, J.; Du, G.; Huang, Y. Feasibility of Piezoceramic Transducer-Enabled Active Sensing for the Monitoring Cross-shaped Concrete Filled Steel Tubular (CCFST) Columns under Cyclic Loading. *Measurement* **2021**, *182*, 109646. [CrossRef]
16. Fan, J.; Lyu, F.; Ding, F.; Bu, D.; Wang, S.; Tan, Z.; Tan, S. Compatibility Optimal Design of Axially Loaded Circular Concrete-Filled Steel Tube Stub Columns. *Materials* **2021**, *14*, 4839. [CrossRef]
17. Reddy, S.V.B.; Sivasankar, S. Axial behaviour of corroded CFST columns wrapped with GFRP sheets—An experimental investigation. In *Advances in Structural Engineering*; Springer: Berlin/Heidelberg, Germany, 2020; pp. 15–28.
18. Teng, J.; Wang, J.; Lin, G.; Zhang, J.; Feng, P. Compressive behavior of concrete-filled steel tubular columns with internal high-strength steel spiral confinement. *Adv. Struct. Eng.* **2021**, *24*, 1687–1708. [CrossRef]
19. Güneyisi, E.M.; Nour, A.I. Axial compression capacity of circular CFST columns transversely strengthened by FRP. *Eng. Struct.* **2019**, *191*, 417–431. [CrossRef]
20. Yu, M.; Zha, X.; Ye, J.; She, C. A unified formulation for hollow and solid concrete-filled steel tube columns under axial compression. *Eng. Struct.* **2010**, *32*, 1046–1053. [CrossRef]
21. Wu, B.; Zhang, Q.; Chen, G. Compressive behavior of thin-walled circular steel tubular columns filled with steel stirrup-reinforced compound concrete. *Eng. Struct.* **2018**, *170*, 178–195. [CrossRef]
22. Abdalla, S.; Abed, F.; AlHamaydeh, M. Behavior of CFSTs and CCFSTs under quasi-static axial compression. *J. Constr. Steel Res.* **2013**, *90*, 235–244. [CrossRef]
23. Xu, L.; Cai, M.; Dong, S.; Yin, S.; Xiao, T.; Dai, Z.; Wang, Y.; Soltanian, M.R. An upscaling approach to predict mine water inflow from roof sandstone aquifers. *J. Hydrol.* **2022**, *612*, 128314. [CrossRef]
24. Seyedashraf, O.; Mehrabi, M.; Akhtari, A.A. Novel approach for dam break flow modeling using computational intelligence. *J. Hydrol.* **2018**, *559*, 1028–1038. [CrossRef]
25. Moayedi, H.; Mehrabi, M.; Mosallanezhad, M.; Rashid, A.S.A.; Pradhan, B. Modification of landslide susceptibility mapping using optimized PSO-ANN technique. *Eng. Comput.* **2019**, *35*, 967–984. [CrossRef]
26. Zhan, C.; Dai, Z.; Soltanian, M.R.; de Barros, F.P. Data-worth analysis for heterogeneous subsurface structure identification with a stochastic deep learning framework. *Water Resour. Res.* **2022**, *58*, e2022WR033241. [CrossRef]
27. Duan, J.; Asteris, P.G.; Nguyen, H.; Bui, X.-N.; Moayedi, H. A novel artificial intelligence technique to predict compressive strength of recycled aggregate concrete using ICA-XGBoost model. *Eng. Comput.* **2020**, *37*, 1–18. [CrossRef]
28. Chandwani, V.; Agrawal, V.; Nagar, R. Modeling slump of ready mix concrete using genetic algorithms assisted training of Artificial Neural Networks. *Expert Syst. Appl.* **2015**, *42*, 885–893. [CrossRef]
29. Nguyen, M.-S.T.; Trinh, M.-C.; Kim, S.-E. Uncertainty quantification of ultimate compressive strength of CCFST columns using hybrid machine learning model. *Eng. Comput.* **2021**, *38*, 1–20. [CrossRef]
30. Tran, V.-L.; Kim, S.-E. Efficiency of three advanced data-driven models for predicting axial compression capacity of CFDST columns. *Thin-Walled Struct.* **2020**, *152*, 106744. [CrossRef]
31. Basarir, H.; Elchalakani, M.; Karrech, A. The prediction of ultimate pure bending moment of concrete-filled steel tubes by adaptive neuro-fuzzy inference system (ANFIS). *Neural Comput. Appl.* **2019**, *31*, 1239–1252. [CrossRef]
32. Ho, N.X.; Le, T.-T. Effects of variability in experimental database on machine-learning-based prediction of ultimate load of circular concrete-filled steel tubes. *Measurement* **2021**, *176*, 109198. [CrossRef]
33. Tran, V.-L.; Thai, D.-K.; Nguyen, D.-D. Practical artificial neural network tool for predicting the axial compression capacity of circular concrete-filled steel tube columns with ultra-high-strength concrete. *Thin-Walled Struct.* **2020**, *151*, 106720. [CrossRef]
34. Zhao, Y.; Zhong, X.; Foong, L.K. Predicting the splitting tensile strength of concrete using an equilibrium optimization model. *Steel Compos. Struct.* **2021**, *39*, 81–93.
35. Lyu, F.; Fan, X.; Ding, F.; Chen, Z. Prediction of the axial compressive strength of circular concrete-filled steel tube columns using sine cosine algorithm-support vector regression. *Compos. Struct.* **2021**, *273*, 114282. [CrossRef]
36. Luat, N.-V.; Shin, J.; Lee, K. Hybrid BART-based models optimized by nature-inspired metaheuristics to predict ultimate axial capacity of CCFST columns. *Eng. Comput.* **2020**, *38*, 1–30.
37. Sarir, P.; Armaghani, D.J.; Jiang, H.; Sabri, M.M.S.; He, B.; Ulrikh, D.V. Prediction of Bearing Capacity of the Square Concrete-Filled Steel Tube Columns: An Application of Metaheuristic-Based Neural Network Models. *Materials* **2022**, *15*, 3309. [CrossRef] [PubMed]
38. Bardhan, A.; Biswas, R.; Kardani, N.; Iqbal, M.; Samui, P.; Singh, M.; Asteris, P.G. A novel integrated approach of augmented grey wolf optimizer and ann for estimating axial load carrying-capacity of concrete-filled steel tube columns. *Constr. Build. Mater.* **2022**, *337*, 127454. [CrossRef]

39. Zheng, Y.; Jin, H.; Jiang, C.; Moradi, Z.; Khadimallah, M.A.; Moayedi, H. Analyzing behavior of circular concrete-filled steel tube column using improved fuzzy models. *Steel Compos. Struct.* **2022**, *43*, 625–637.
40. Jang, J.-S. ANFIS: Adaptive-network-based fuzzy inference system. *IEEE Trans. Syst. Man Cybern.* **1993**, *23*, 665–685. [CrossRef]
41. Ebrahimi-Khusfi, Z.; Taghizadeh-Mehrjardi, R.; Nafarzadegan, A.R. Accuracy, uncertainty, and interpretability assessments of ANFIS models to predict dust concentration in semi-arid regions. *Environ. Sci. Pollut. Res.* **2021**, *28*, 6796–6810. [CrossRef] [PubMed]
42. Alajmi, M.S.; Almeshal, A.M. Prediction and optimization of surface roughness in a turning process using the ANFIS-QPSO method. *Materials* **2020**, *13*, 2986. [CrossRef]
43. Moayedi, H.; Mehrabi, M.; Kalantar, B.; Abdullahi Mu'azu, M.; A. Rashid, A.S.; Foong, L.K.; Nguyen, H. Novel hybrids of adaptive neuro-fuzzy inference system (ANFIS) with several metaheuristic algorithms for spatial susceptibility assessment of seismic-induced landslide. *Geomat. Nat. Hazards Risk* **2019**, *10*, 1879–1911. [CrossRef]
44. Yang, X.-S. Metaheuristic optimization. *Scholarpedia* **2011**, *6*, 11472. [CrossRef]
45. Yang, X.-S. Metaheuristic optimization: Algorithm analysis and open problems. In Proceedings of the International Symposium on Experimental Algorithms, Crete, Greece, 5–7 May 2011; Springer: Berlin/Heidelberg, Germany, 2011; pp. 21–32.
46. Moayedi, H.; Mehrabi, M.; Bui, D.T.; Pradhan, B.; Foong, L.K. Fuzzy-metaheuristic ensembles for spatial assessment of forest fire susceptibility. *J. Environ. Manag.* **2020**, *260*, 109867. [CrossRef] [PubMed]
47. Wang, G.-G.; Deb, S.; dos Santos Coelho, L. Earthworm optimisation algorithm: A bio-inspired metaheuristic algorithm for global optimisation problems. *IJBIC* **2018**, *12*, 1–22. [CrossRef]
48. Ghosh, I.; Roy, P.K. Application of earthworm optimization algorithm for solution of optimal power flow. In Proceedings of the 2019 International Conference on Opto-Electronics and Applied Optics (Optronix), Kolkata, India, 18–20 March 2019; IEEE: New York, NY, USA, 2019; pp. 1–6.
49. Kanna, S.R.; Sivakumar, K.; Lingaraj, N. Development of Deer Hunting linked Earthworm Optimization Algorithm for Solving large scale Traveling Salesman Problem. *Knowl. Based Syst.* **2021**, *227*, 107199. [CrossRef]
50. Eberhart, R.; Kennedy, J. A new optimizer using particle swarm theory, MHS'95. In Proceedings of the Sixth International Symposium on Micro Machine and Human Science, Nagoya, Japan, 4–6 October 1995; IEEE: New York, NY, USA, 1995; pp. 39–43.
51. Nguyen, H.; Mehrabi, M.; Kalantar, B.; Moayedi, H.; Abdullahi, M.a.M. Potential of hybrid evolutionary approaches for assessment of geo-hazard landslide susceptibility mapping. *Geomat. Nat. Hazards Risk* **2019**, *10*, 1667–1693. [CrossRef]
52. Mehrabi, M.; Pradhan, B.; Moayedi, H.; Alamri, A. Optimizing an adaptive neuro-fuzzy inference system for spatial prediction of landslide susceptibility using four state-of-the-art metaheuristic techniques. *Sensors* **2020**, *20*, 1723. [CrossRef]
53. Poli, R.; Kennedy, J.; Blackwell, T. Particle swarm optimization. *Swarm Intell.* **2007**, *1*, 33–57. [CrossRef]
54. Mirjalili, S.; Gandomi, A.H.; Mirjalili, S.Z.; Saremi, S.; Faris, H.; Mirjalili, S.M. Salp Swarm Algorithm: A bio-inspired optimizer for engineering design problems. *Adv. Eng. Softw.* **2017**, *114*, 163–191. [CrossRef]
55. Tubishat, M.; Ja'afar, S.; Alswaitti, M.; Mirjalili, S.; Idris, N.; Ismail, M.A.; Omar, M.S. Dynamic salp swarm algorithm for feature selection. *Expert Syst. Appl.* **2021**, *164*, 113873.
56. Ye, X.; Moayedi, H.; Khari, M.; Foong, L.K. Metaheuristic-hybridized multilayer perceptron in slope stability analysis. *Smart Struct. Syst.* **2020**, *26*, 263–275.
57. Rao, R.V.; Savsani, V.J.; Vakharia, D. Teaching–learning-based optimization: A novel method for constrained mechanical design optimization problems. *Comput. Aided Des.* **2011**, *43*, 303–315. [CrossRef]
58. Zhao, Y.; Bai, C.; Xu, C.; Foong, L.K. Efficient metaheuristic-retrofitted techniques for concrete slump simulation. *Smart Struct. Syst.* **2021**, *27*, 745–759.
59. Chen, W.; Chen, X.; Peng, J.; Panahi, M.; Lee, S. Landslide susceptibility modeling based on ANFIS with teaching-learning-based optimization and Satin bowerbird optimizer. *Geosci. Front.* **2021**, *12*, 93–107. [CrossRef]
60. Ghoneim, S.S.; Mahmoud, K.; Lehtonen, M.; Darwish, M.M. Enhancing Diagnostic Accuracy of Transformer Faults Using Teaching-Learning-Based Optimization. *IEEE Access* **2021**, *9*, 30817–30832. [CrossRef]
61. Mehrabi, M. Landslide susceptibility zonation using statistical and machine learning approaches in Northern Lecco, Italy. *Nat. Hazards* **2021**, *11*, 1–37. [CrossRef]
62. Mehrabi, M.; Moayedi, H. Landslide susceptibility mapping using artificial neural network tuned by metaheuristic algorithms. *Environ. Earth Sci.* **2021**, *80*, 1–20. [CrossRef]